Improved force field of (E)-1,3,5-hexatriene based on deuteriated derivatives

Langkilde, F.W.; Wilbrandt, R.; Brouwer, A.M.

Published in:
Journal of Physical Chemistry

DOI:
10.1021/j100375a013

the charge-transfer absorption. These wave patterns could be the result of a localized-to-delocalized transition in the absorbing singlet manifold. This theory is currently being tested and will be the subject of a future report.

Conclusions

Energy levels in a phen chromophore are particularly sensitive to electron-donating substituents in the 4,7 positions. Other substituent groups in these positions should lead to a series of interesting tunable mixed-ligand species.

Coupling between near-degenerate localized states in a mixed-ligand complex produces results consistent with the ICC model. Selection of the energy separation of MLCT states of different chromophores should allow the design of molecules with variable P_{max} values that may extend from a lower limit of approximately 0.23 to near the maximum possible P of 0.5 in a continuous fashion. Also, the proportion of excited molecules in each Ru-L state may be selected by appropriately varying the energy of the π^* orbitals. Because the localized states are not in a thermal equilibrium with one another on the time scale of the luminescence, this proportion should be relatively insensitive to temperature.

Acknowledgment. This work was supported by the Army Research Office (Grant No. DAAL-03-86-K-0040).

Improved Force Field of (*E*)-1,3,5-Hexatriene Based on Deuteriated Derivatives

Frans W. Langkilde,*

Department of Physical Chemistry A, Royal Danish School of Pharmacy, 2 Universitetsparken, DK-2100 Copenhagen, Denmark

Robert Wilbrandt,

Chemistry Department, Risø National Laboratory, DK-4000 Roskilde, Denmark

and Albert M. Brouwer

Laboratory of Organic Chemistry, University of Amsterdam, NL-1018 WS Amsterdam, The Netherlands
(Received: October 9, 1989; In Final Form: January 9, 1990)

Raman and infrared spectra of ground-state (*E*)-1,3,5-hexatriene-*3,4-d*$_2$ (d34EHT), (*E*)-1,3,5-hexatriene-*3-d* (d3EHT), (*E*)-1,3,5-hexatriene-*1,1-d*$_2$ (d11EHT), and (*E*)-1,3,5-hexatriene-*2,5-d*$_2$ (d25EHT) are reported. Together with previously published spectra of (*E*)-1,3,5-hexatriene (EHT), these spectra are used to refine a scaled ab initio force field from the literature, calculated at the HF/6-31G level, and the spectra of EHT, d34EHT, d3EHT, d11EHT, and d25EHT are interpreted by use of the resulting refined force field. The changes in the force field are discussed, as are the changes in normal modes upon deuteriation.

Introduction

Vibrational analysis of 1,3,5-hexatriene has been a matter of interest since Lippincott's early reports.[1,2] We have studied the vibrations of 1,3,5-hexatriene and methylated derivatives both in the ground state[3,4] and in the lowest excited triplet state.[5-9] The analysis of excited-state vibrational spectra is difficult, since the knowledge of geometry and bond properties in excited states is limited. One effort to understand the excited-state vibrations is the investigation of excited states of isotopically substituted compounds, and we have started work in this direction.[9] Another effort is the correlation between excited-state and ground-state vibrations, although it should be applied with caution due to the rotation of normal modes (Duschinsky effect). Here, it is important that the vibrational analysis of the ground state is complete and correct. Consequently, isotopically substituted compounds should be investigated in the ground state as well.

Recently, four groups have published calculations on the vibrations of (*E*)-1,3,5-hexatriene: Hemley et al. (HBK),[10] Bock et al. (BPKP),[11] Fogarasi et al. (FSLBP),[12] and Yoshida et al. (YFT).[13] Furthermore, a detailed study of the influence of electron correlation on the force field of the in-plane vibrations has appeared (SKL).[14] The calculations by HBK are semiempirical, whereas the latter four are ab initio. The results of

(1) Lippincott, E. R.; White, C. E.; Sibilia, J. P. *J. Am. Chem. Soc.* **1958**, *80*, 2926.
(2) Lippincott, E. R.; Kenney, T. E. *J. Am. Chem. Soc.* **1962**, *84*, 3641.
(3) Langkilde, F. W.; Wilbrandt, R.; Nielsen, O. F.; Christensen, D. H.; Nicolaisen, F. M. *Spectrochim. Acta* **1987**, *43A*, 1209.
(4) Langkilde, F. W.; Amstrup, B.; Wilbrandt, R.; Brouwer, A. M. *Spectrochim. Acta* **1989**, *45A*, 883.
(5) Langkilde, F. W.; Wilbrandt, R.; Jensen, N.-H. *Chem. Phys. Lett.* **1984**, *111*, 372.
(6) Langkilde, F. W.; Jensen, N.-H.; Wilbrandt, R. *Chem. Phys. Lett.* **1985**, *118*, 486.
(7) Langkilde, F. W.; Jensen, N.-H.; Wilbrandt, R.; Brouwer, A. M.; Jacobs, H. J. C. *J. Phys. Chem.* **1987**, *91*, 1029.
(8) Langkilde, F. W.; Jensen, N.-H.; Wilbrandt, R. *J. Phys. Chem.* **1987**, *91*, 1040.
(9) Negri, F.; Orlandi, G.; Brouwer, A. M.; Langkilde, F. W.; Wilbrandt, R. *J. Chem. Phys.* **1989**, *90*, 5944.
(10) Hemley, R. J.; Brooks, B. R.; Karplus, M. *J. Chem. Phys.* **1986**, *85*, 6550.
(11) Bock, C. W.; Panchenko, Y. N.; Krasnoshchiokov, S. V.; Pupyshev, V. I. *J. Mol. Struct.* **1986**, *148*, 131.
(12) Fogarasi, G.; Szalay, P. G.; Liescheski, P. P.; Boggs, J. E.; Pulay, P. *J. Mol. Struct.* **1987**, *151*, 341.
(13) Yoshida, H.; Furukawa, Y.; Tasumi, M. *J. Mol. Struct.* **1989**, *194*, 279.
(14) Szalay, P. G.; Karpfen, A.; Lischka, H. *J. Chem. Phys.* **1987**, *87*, 3530.

0022-3654/90/2094-4809$02.50/0

the calculations differ in several respects, among which are the frequencies of the normal modes that are dominated by C=C stretches, the frequencies of the normal modes dominated by CH rocks, the frequency of the b_u symmetry normal mode dominated by C–C stretches, and the frequencies of the normal modes dominated by CH and CH_2 out-of-plane wags. However, the agreement of the ab initio calculations with each other and with experiment is generally better than for the semiempirical calculation.

The experimental basis for these calculations consists of infrared and Raman spectra of (*E*)-1,3,5-hexatriene[1-3,13,15,16] and one isotopically substituted derivative: (*E*)-1,3,5-hexatriene-*2,3,4,5-d*$_4$ (d2345EHT).[16,17] Whereas the vibrational spectra of (*E*)-1,3,5-hexatriene are now well established, as seen from the agreement between the most recent experimental results,[3,13] those of d2345EHT are incomplete. In comparison, the vibrational spectra of 1,3-butadiene have been interpreted on the basis of the parent compound and as many as 11 deuteriated derivatives.

For the above reasons, we found it important to investigate additional deuteriated analogues of (*E*)-1,3,5-hexatriene (EHT). We have recently published the ground-state Raman and preresonance Raman spectra of (*E*)-1,3,5-hexatriene-*3,4-d*$_2$ (d34EHT) and the preresonance Raman spectrum of (*E*)-1,3,5-hexatriene-*2,5-d*$_2$ (d25EHT).[9] In the present paper we report the ground-state Raman and Fourier transform (FT) infrared spectra of d34EHT, (*E*)-1,3,5-hexatriene-*3-d* (d3EHT), and (*E*)-1,3,5-hexatriene-*1,1-d*$_2$ (d11EHT). These spectra are used together with the previously published spectra of EHT[3,13] to establish a force field.

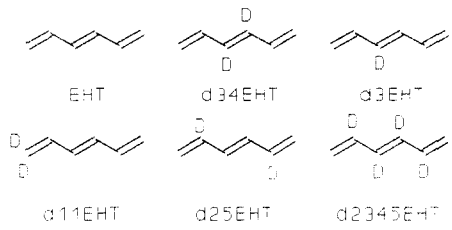

Among these, EHT, d34EHT, d25EHT, and d2345EHT transform according to C_{2h} symmetry and so obey the exclusion principle between Raman and infrared-active vibrational transitions; d3EHT and d11EHT transform according to C_s symmetry.

Materials

The synthesis of (*E*)-1,3,5-hexatriene-*3,4-d*$_2$ and (*E*)-1,3,5-hexatriene-*2,5-d*$_2$ has been described previously.[9] (*E*)-1,3,5-Hexatriene-*3-d* was prepared by reduction of 3-hexyne-2,5-diol with lithium aluminum hydride/D_2O,[9] acetylation, and elimination of acetic acid using palladium(II) acetate and triphenylphosphine in toluene.[18] This method is far superior to the pyrolysis we used earlier.[9] From the mixture of triene and toluene thus obtained small samples were isolated by use of preparative gas chromatography (Varian 2700, Ucon column, He carrier gas, 60 °C). (*E*)-1,3,5-Hexatriene-*1,1-d*$_2$ was synthesized starting from (*E*,*E*)-2,4-hexadienoic acid. Reduction with $LiAlD_4$ in ether/THF afforded hexa-2,4-dien-1-ol-*1,1-d*$_2$, which was acetylated and converted to the triene as described above. The purified samples were distilled into glass capillaries under reduced pressure. The capillaries were cooled briefly, sealed, and kept in a freezer.

Capillary gas chromatography (DB225 column, 30–55 °C, carrier gas He) showed the sample of d3EHT to contain 98% of the *E* isomer and 2% of the *Z* isomer and the sample of d11EHT to contain 96% of the *E* isomer and 4% of the *Z* isomer, whereas for d34EHT and d25EHT no isomeric or other impurities were found. A high deuterium content (>95%) of the deuteriated products was indicated by ^1H NMR spectrometery (Bruker WM300, 300 MHz).

Experimental Methods

The Raman spectra were obtained of the samples in the capillary glass tubes, with outer diameter 3 (d34EHT and d11EHT) or 4 mm (d3EHT), thermostated at 10 °C. Afterward, the samples were transferred under argon to a vacuum line and from this to spectroscopic cells for gas-phase FT-infrared spectra at room temperature.

The Raman and FT-infrared spectrometers have been described in detail previously.[3,4] Raman spectra were recorded in the region 3400–10 cm^{-1} with 514.5-nm excitation. Perpendicular illumination with vertically polarized light was used in a horizontal scattering plane; spectra were obtained in I_{VV} and I_{VH} configurations. The spectral slit width was 2.9 cm^{-1} or less.

Mid infrared spectra were obtained in the region 4000–500 cm^{-1} with a resolution of 0.5 cm^{-1}. A Ge/KBr beam splitter and a liquid nitrogen cooled MCT detector with KBr windows were used. The spectroscopic cell was a 10-cm gas cell with KBr windows. For d34EHT and d3EHT, infrared spectra were obtained in the region 700–50 cm^{-1}, with 1-cm^{-1} resolution, a 3.5-μm Myler beam splitter, a room temperature DTGS detector with polyethylene (PE) windows, and a 20-cm cell with PE windows. For d11EHT, an infrared spectrum was obtained in the region 700–300 cm^{-1}, with 1-cm^{-1} resolution, a Ge/KBr beam splitter, the DTGS detector, and a 10-cm cell with KBr windows.

Experimental Results

The Raman spectra of neat d3EHT and d11EHT are shown in Figures 1 and 2, respectively. For d34EHT and d25EHT, the Raman spectra and their experimental conditions are found in ref 9. For d25EHT, the Raman spectrum was only obtained in connection with time-resolved resonance Raman studies of the lowest excited triplet state,[9] from acetonitrile solution with 317.5-nm excitation, and only the strongest Raman bands were observed. Due to a very limited amount of sample of d25EHT, we could not obtain in full Raman and infrared spectra of this compound. The infrared and Raman spectra of EHT, and their experimental conditions, are found in ref 3. The Raman spectra in the $R(\bar{\nu})$ representation[4,19] of the region below 400 cm^{-1} are shown in parts A, B, and C of Figure 3 for d34EHT, d3EHT, and d11EHT, respectively. The infrared spectra of d34EHT, d3EHT, and d11EHT are only listed in the tables (see below); however, they are available on request.

The wavenumbers, intensities, and depolarization ratios of Raman bands, and wavenumbers, intensities, and band contours of infrared bands, are listed in Tables I, II, and III for d34EHT, d3EHT, and d11EHT, respectively, together with calculated frequencies and potential energy distributions (PED) of the normal modes (see below). The Raman wavenumbers, intensities, and depolarization ratios listed in Tables I–III for bands below 400 cm^{-1} were obtained from the $R(\bar{\nu})$ spectra. For d25EHT, the wavenumbers and intensities of Raman bands are listed in Table IV, together with calculated frequencies and PED of the normal modes. The experimentally observed wavenumbers of fundamentals of EHT from ref 3 are listed in Table V, together with calculated frequencies and PED of the normal modes from the present study.

If one accepts the view proposed previously[3] that the observed EHT Raman bands at 1637 and 1623 cm^{-1} are due to a Fermi resonance between an 1188 + 444 cm^{-1} combination and the +++ C=C stretching mode, the unperturbed +++ mode is predicted at 1628 cm^{-1}. This value is entered in Table V. The value observed previously by us for the highest wavenumber C=C torsion of b_g symmetry (428 cm^{-1})[3] is too far from the calculated value (612 cm^{-1}) and has been replaced in Table V by the frequency observed in the crystalline phase in a later study (615 cm^{-1}).[13]

(15) McDiarmid, R.; Sabljic, A. *J. Phys. Chem.* **1987**, *91*, 276.
(16) Rakovic, D.; Stepanyan, S. A.; Gribov, L. A.; Panchenko, Y. N. *J. Mol. Struct.* **1982**, *90*, 363.
(17) Panchenko, Y. N.; Pentin, Y. A.; Rusach, E. B. *Russ. J. Phys. Chem.* **1975**, *49*, 1536.
(18) Yamamoto, K.; Suzuki, S.; Tsuji, J. *Bull. Chem. Soc. Jpn.* **1981**, *54*, 2541.
(19) Nielsen, O. F.; Lund, P.-A.; Præstgaard, E. *J. Chem. Phys.* **1982**, *77*, 3878.

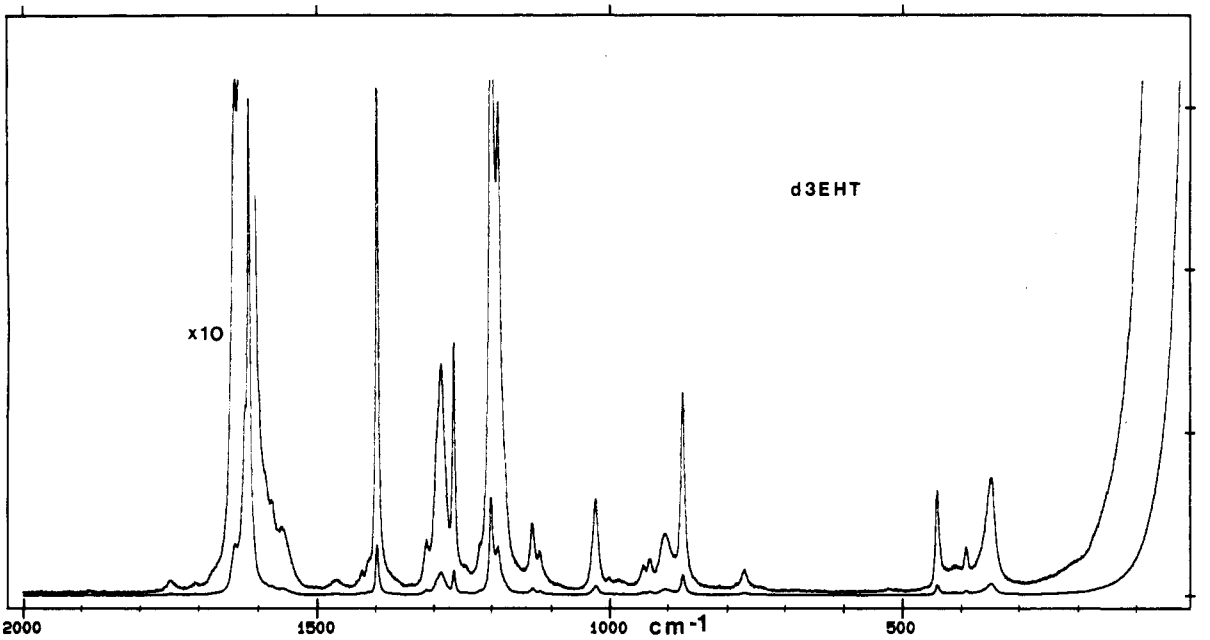

Figure 1. Raman spectrum of neat (*E*)-1,3,5-hexatriene-*3-d* (d3EHT) at 10 °C, I_{VV} configuration.

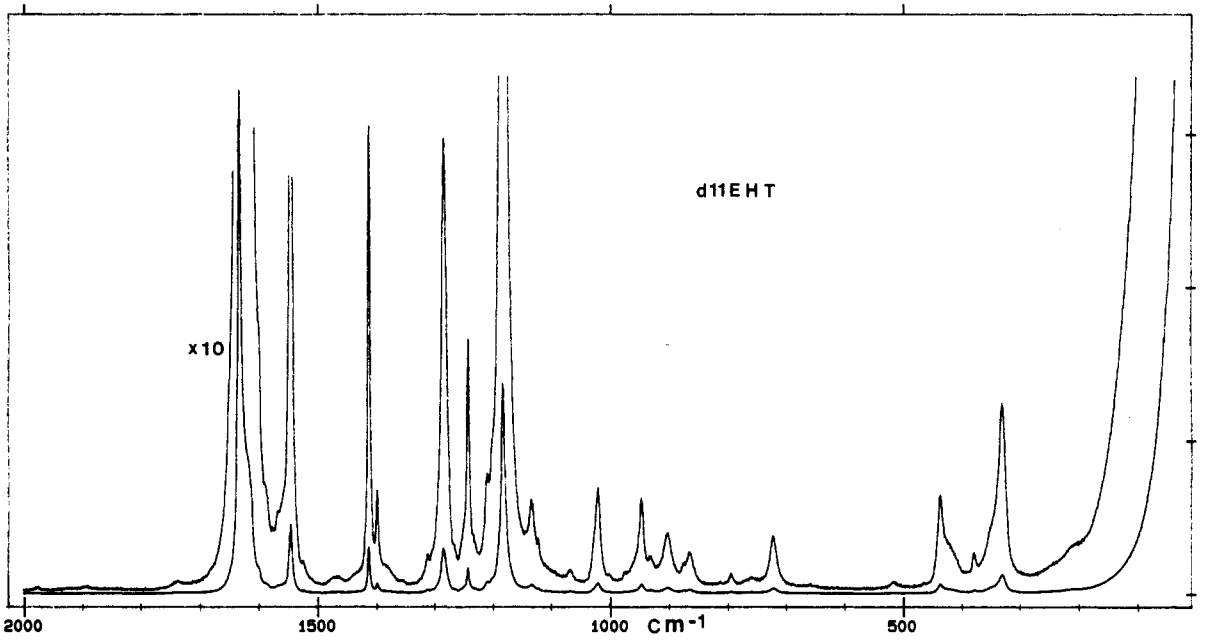

Figure 2. Raman spectrum of neat (*E*)-1,3,5-hexatriene-*1,1-d*$_2$ (d11EHT) at 10 °C, I_{VV} configuration.

For the region 3400–2000 cm^{-1}, only those Raman and infrared bands are reported that may possibly be attributed to CH or CD stretch fundamentals. This is done in Table VI for the four compounds EHT, d34EHT, d3EHT, and d11EHT. In Table VII, these CH and CD stretches are assigned to the calculated frequencies and the PED of the normal modes are listed.

Theoretical Methods

In the analysis of the observed vibrational spectra we used two computer programs, VIBROT and FLINDA,[20] both based on a valence force field. FLINDA is used to refine a valence force field from starting values of the force constants. The input consists of the molecular geometry, the internal coordinates, the nuclear masses, the experimentally observed frequencies, and starting values for the valence force field. For each force constant, it is specified whether it should be kept fixed or varied in the refinement. By least-squares analysis, FLINDA iterates a new force field.

VIBROT subsequently calculates the wavenumbers and internal-coordinate compositions of the normal modes from the molecular geometry, the internal coordinates, the nuclear masses, and the refined valence force field. The VIBROT and FLINDA calculations were carried out on an RC 8000 computer.

With respect to the equilibrium molecular structure of (*E*)-1,3,5-hexatriene a choice has to be made: On the one hand, the only experimental study of the geometry of EHT (gas-phase electron diffraction) is more than 20 years old;[21] on the other hand, the geometry has been calculated theoretically in several recent studies, using mainly ab initio methods.[10-14,22-25] The theoretical geometries agree well with each other, but the agreement between the theoretical geometries on one side and the experimental one

(20) Bjørklund, S.; Augdahl, E.; Christensen, D. H.; Sørensen, G. O. *Spectrochim. Acta* **1976**, *32A*, 1021.

(21) Trætteberg, M. *Acta Chem. Scand.* **1968**, *22*, 628.
(22) Hess, B. A.; Schaad, L. J. *J. Am. Chem. Soc.* **1983**, *105*, 7500.
(23) Kirtman, B.; Nilsson, W. B.; Palke, W. E. *Solid State Commun.* **1983**, *46*, 791.
(24) Häfelinger, G.; Regelmann, C. U.; Krygowski, T. M.; Wozniak, K. *J. Comput. Chem.* **1989**, *10*, 329.
(25) Bock, C. W.; George, P.; Trachtman, M. *J. Mol. Struct.* **1984**, *109*, 1.

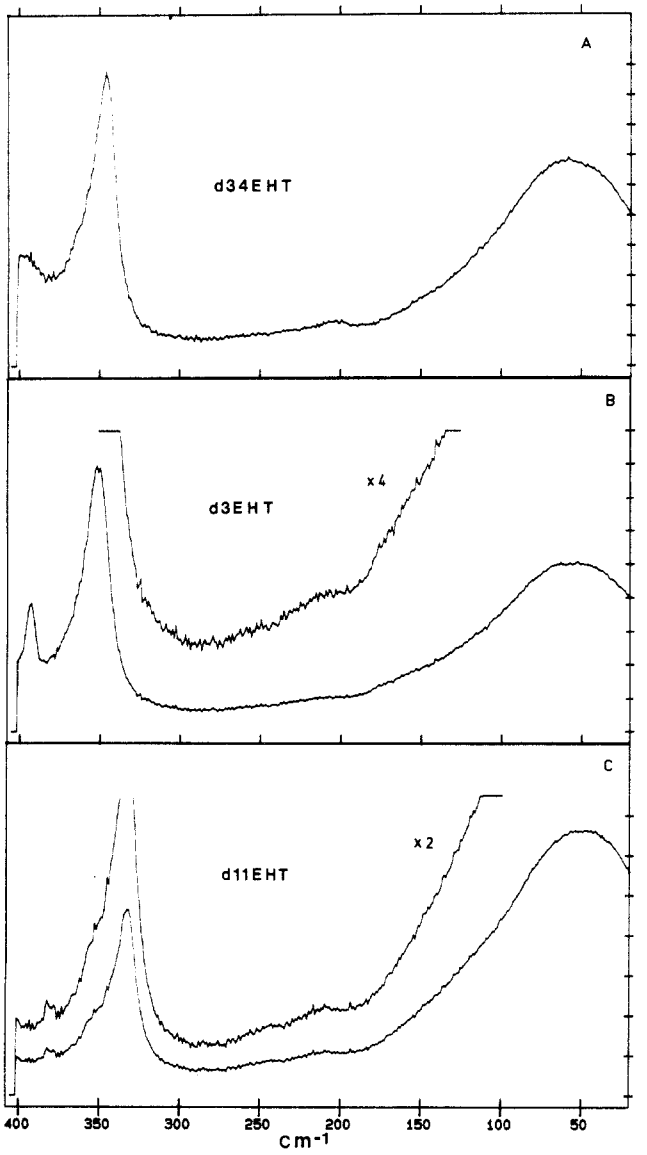

Figure 3. Raman R($\bar{\nu}$) spectra of neat (*E*)-1,3,5-hexatriene-*3,4-d*$_2$ (d34EHT) (A), (*E*)-1,3,5-hexatriene-*3-d* (d3EHT) (B), and (*E*)-1,3,5-hexatriene-*1,1-d*$_2$ (d11EHT) (C) at 10 °C, I_{VV} configuration.

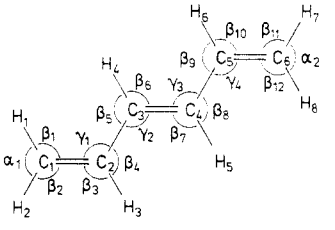

Figure 4. Atom numbering and internal coordinates of (*E*)-1,3,5-hexatriene and deuteriated derivatives.

on the other is poor. Consequently, we have to choose between the experimental and theoretical geometries.

The differences between theory and experiment are discussed at length in FSLBP and SKL, especially with respect to the relative lengths of the terminal and central C=C bonds. We find the agreement among the theoretical geometries striking, although it can partly be explained by the fact that some of the studies use very similar methods. In conclusion, we favor the theoretical geometries. Among the values of the geometrical parameters from the different theoretical studies, we choose typical values, close to those of BPKP and YFT. These are listed in Table VIII, together with the experimental ones. The atom numbering is given in Figure 4. It is seen from Table VIII that the disagreement between theory and experiment is significant and concerns important geometrical parameters, especially the length of the central C=C bond. The internal coordinates used in the present study are defined in Figure 4 and Table IX. They are identical with those of BPKP, although our numbering is different. (Although we use the term internal coordinates, the coordinates in Table IX are strictly speaking group coordinates.)

As mentioned above, d3EHT and d11EHT transform according to C_h symmetry. For this reason, we performed the calculations for all molecules investigated under the assumption of C_h symmetry, i.e., with the in-plane vibrations of a′ symmetry and the out-of-plane vibrations of a″ symmetry. The experimental frequencies used for d3EHT and d11EHT, where vibrations may be both Raman and infrared active, were mostly Raman values.

The starting values in the iteration of the refined valence force field were taken from BPKP. The iteration was carried out using the experimentally observed frequencies for EHT, d34EHT, d3EHT, and d11EHT.

Theoretical Results

The calculated wavenumbers and potential energy distributions of the normal modes are listed in Tables I, II, III, and V for d34EHT, d3EHT, d11EHT, and EHT, respectively. The same is done in part for d25EHT in Table IV. The PED are calculated as the square of the coefficient of an internal coordinate in a normal mode, multiplied by the pertinent diagonal force constant. However, the sign of the coefficients is retained in the PED, as listed in Tables I–V. Only the dominant internal coordinates are shown; they appear in order of the size of their contribution. The calculated wavenumbers and PED of the CH and CD stretches are listed in Table VII for the four compounds EHT, d34EHT, d3EHT, and d11EHT and assigned to the observed bands from Table VI. The calculated wavenumbers and the symmetry of normal modes are summarized in Table X for EHT, d34EHT, d3EHT, d11EHT, and d25EHT, together with the observed values.

For the in-plane vibrations, only 19 force constants were changed in the iteration: The 13 diagonal ones, 1 C–H stretch–stretch coupling constant, and 5 coupling constants for the interaction between CC stretches. Our final refined values are listed in Table XI, together with the starting ones from BPKP, and those of YFT,[28] FSLBP, and SKL.

For the out-of-plane vibrations, a large part of the force constants were refined. The refined force field is listed on Table XII, together with those of BPKP, YFT, and FSLBP.

Discussion

Deuterium substitution in (*E*)-1,3,5-hexatriene has two general effects on the molecular vibrations. First, it shifts downward the frequency of the vibrations where hydrogen is directly involved: CH stretch, CH in-plane rock, CH out-of-plane wag. Second, it decouples the CH vibrations being deuteriated from other vibrations of similar frequencies and induces new couplings with vibrations at lower frequencies, causing the whole vibrational pattern to change.

Most of the fundamentals are assigned unambiguously in the experimental spectra in Tables I–V and VII. All C=C and C–C stretches of the four compounds EHT, d34EHT, d3EHT, and d11EHT are described well by our calculations. This also applies to the CH_2 (CD_2) scissorings and in-plane rocks and the CCC deformations. The discrepancies between theory and experiment are slightly larger for the CH (CD) in-plane rocks. This may be partly explained by the fact that our calculations do not take anharmonicity into account. The out-of-plane modes are generally described very well. The largest discrepancies are found for d34EHT and d3EHT for out-of-plane CH wags (d34EHT, 999 cm^{-1}; d3EHT, 1002 and 987 cm^{-1}; calculated).

However, in a few cases the assignment is doubtful; these cases shall be mentioned here. In Table I for d34EHT, the observed

(26) Wilson, E. B.; Decius, J. C.; Cross, P. C. *Molecular Vibrations*; McGraw-Hill: New York, 1955.
(27) Morino, Y.; Shimanouchi, T. *Pure Appl. Chem.* **1978**, *50*, 1707.
(28) Tasumi, M. Private communication.

TABLE I: Observed Wavenumbers (cm^{-1}) and Depolarization Ratios of Raman Bands and Wavenumbers and Band Contours of Infrared Bands of (*E*)-1,3,5-Hexatriene-*3,4-d*$_2$ in the Region 2000–10 cm^{-1}, Together with Calculated Wavenumbers and Potential Energy Distributions of Normal Modes[a]

Raman (liquid)	I_{VH}/I_{VV}	infrared (gas) R	Q	P	contour	calc wavenumber	calc PED[b]
		1974		1965	w B		
1913 w	P						
		1901	1892	1882	w		
		1814	1809	1805	s A		
			1782		m		
1741 w	0.31						
		1734		1726	m A/B		
1638 m	0.32						
1629 sh	P						
		1628	1623	1619	s A	1623	5 - 18
1607 s	0.17					1607	7 + 5 + 18
1591 m	0.25						
1565 s	0.34					1563	7 - 5 - 18 - 8 - 20
		1563		1553	m A/B		
1548 m	0.32						
		1525		1516	m A/B		
1461 w	0.49						
		1458		1448	w A/B		
1438 w	0.59						
		1429	1425	1419	m A	1427	8 - 20
1424 w	0.39						
1396 s	0.26					1394	8 + 20
		1378		1370	w A/B		
1344 w	0.35						
		1298	1294	1290	m A	1291	11 - 23
		1290		1281	m B		
1285 s	0.21					1291	11 + 23
1267 sh	0.20						
			1243		w		
1201 s	0.37					1203	6 + 19 - 12 - 24
		1198		1189	w B		
			1184	1177	w		
1171 sh	0.44						
		1137	(1133)	1129	m B	1140	6 - 19 - 9 + 21 + 11 - 23
1131 w	0.53						
		1095		1084	w B		
			1070		w		
		1048	1044	1037	w A	1033	13 - 25 + 6 - 19
1025 w	0.32						
1001 s	0.21					1000	9 + 21 + 13 + 25
		1000	992	983	s C	999	30 + 31 + 35 + 36
984 sh	dp					986	30 - 31 + 35 - 36
954 w	0.24						
925 w	0.45						
		910	902	894	s C	900	32 + 33
901 m	0.77					903	32 - 33
						875	13 - 25 - 9 + 21
871 s	0.37					861	13 + 25 - 9 - 21 - 6 - 19
		851	(846)	841	w B	875?	13 - 25 - 9 + 21
		828		816	w		
			808	800	w		
787 m	0.73					789	28 - 29
		748	736	722	w C	734	28 + 29 + 34
736 w	0.34						
		666	658	648	s C	656	34 - 35 - 36
657 w	P						
558 w	0.79					561	28 - 29 - 35 + 36
		517	(512)	506	m A/B	513	10 - 22 + 12 - 24
		472		461	w B		
438 m	0.09					434	12 + 24 + 6 + 19
			420		w		
395 w	0.49						
360 sh	0.58						
345 m	0.40					342	10 + 22
			342		w		
			247		w	247	34 + 26 + 27
201 w	0.70					202	26 - 27
			151		m	152	12 - 24 - 10 + 22
			87		w	86	26 + 27 - 34
58 m	dp						intermolecular

[a] s = strong, m = medium, w = weak, sh = shoulder; P = polarized, dp = depolarized. Values in parentheses indicate average values referred to in text. [b] PED = potential energy distributions of normal modes; only the dominant internal-coordinate contributions are shown. For the numbering of internal coordinates, see Table IX and Figure 4.

TABLE II: Observed Wavenumbers (cm^{-1}) and Depolarization Ratios of Raman Bands and Wavenumbers and Band Contours of Infrared Bands of (*E*)-1,3,5-Hexatriene-*3-d* in the Region 2000–10 cm^{-1}, Together with Calculated Wavenumbers and Potential Energy Distributions of Normal Modes[a]

Raman (liquid)	I_{VH}/I_{VV}	infrared (gas) R	Q	P	contour	calc wavenumber	calc PED
1970 w	P	1979		1970	w B		
1923 w	P						
1887 w	P						
1864 w	P						
		1813	1809	1805	m A		
			1784		w		
1749 w	0.33						
1707 w	0.48						
1681 sh	P						
1639 s	0.31						
1622 s	P	1632	1628	1623	s A	1626	18 - 5 - 19
1616 s	0.21					1616	5 + 7 - 6
1588 sh	P						
1575 w	P						
1559 m	0.34	1574		1564	w A/B	1571	7 - 18 - 5 - 20 - 8
			1530		w		
1467 w	0.36		1469		w		
1423 w	0.34	1433	1428	1424	m A	1429	8 - 20
1410 sh	P						
1397 s	0.28					1394	20 + 8 - 23
1313 w	0.29						
1296 sh	0.23	1300		1288	m B	1293	11 - 5 + 9
1288 m	0.22					1291	23 - 18 + 21
1266 m	0.14	1273		1262	w B	1267	25 + 7
1247 w	0.24		1250		w		
1221 sh	P						
1203 s	0.36	1208		1199	w B	1204	19 - 21 + 6 - 24
1191 s	0.38						
1132 m	0.36	1135		1126	m A/B	1136	6 - 9 + 11 - 19
1120 w	0.40						
			1104		w		
1089 w	P						
1024 m	0.29					1021	13 + 9
		1017	1009		C	1002	31 + 30 + 36
1001 w	P						
985 w	0.80		996	986	s C	987	30 + 35 - 31
943 w	0.68						
932 w	P		938		w Q	943	21 + 19
921 sh	dp						
905 m	0.76	915	909		s C	906	33 + 29
			902		s C	901	32 + 35
			901		Q		
			895		Q	895	29 - 33
875 m	0.42		875		w Q	868	13 - 9 - 6
		817	808		w C		
			803		w Q		
770 w	0.78	780	770	761	w C	771	28
740 sh							
684 w	dp		681		m C	680	36 + 35 - 31
			596		w		
			580		w	575	28 - 35 + 36 + 30
			564		w		
		545			w		
525 w	P	532		521	m A/B	528	22 - 10 - 12
441 m	0.11					437	24 + 12 + 19 + 6
441 w	dp?						
392 w	P						
364 sh	P						
350 m	0.41					345	10 + 22
252 w			249		w	251	34 + 26 + 27
213 w						208	27 - 26
156 sh			151		w	153	12 - 24 - 10 + 22
83 sh						86	26 + 27 - 34
56 m							intermolecular

[a] Q = Q branch. For further comments, see Table I.

infrared band around 846 cm^{-1} is not likely to represent the calculated 875-cm^{-1} normal mode, because of the large discrepancy between theory and experiment. The 875-cm^{-1} (calculated) band is probably not observed but is hidden under the strong 902-cm^{-1} (observed) band. In Table II for d3EHT, the band calculated at 575 cm^{-1} may be assigned to any of the observed infrared bands at 596, 580, 564, and 545 cm^{-1}, so for this band the agreement between theory and experiment cannot be determined.

For the CH and CD stretches in Table VII, we find some modes where the difference between theory and experiment is rather large: For EHT at 3037 and 3019 cm^{-1} and for d34EHT at 3037 cm^{-1} (a_g symmetry, calculated values). The discrepancy may be partly explained by the fact that the Raman spectra were obtained from the liquid phase, whereas the infrared spectra were obtained

TABLE III: Observed Wavenumbers (cm^{-1}) and Depolarization Ratios of Raman Bands and Wavenumbers and Band Contours of Infrared Bands of (*E*)-1,3,5-Hexatriene-*1,1-d*$_2$ in the Region 2000–10 cm^{-1}, Together with Calculated Wavenumbers and Potential Energy Distributions of Normal Modes

Raman (liquid)	I_{VH}/I_{VV}	infrared (gas) R	Q	P	contour	calc wavenumber	calc PED
1976 w	P						
		1962		1953	w B		
1923 w	P						
1893 w	P						
		1884		1875	w B		
		1864		1856	m B		
		1830	1825		w		
		1811		1803	m B		
			1781		w		
		1770		1760	w A/B		
1738 w	P						
1633 s	0.21	1641	1637	1633	m A	1630	7 + 18 − 19
1617 sh	P	1622	1618	1613	s A	1612	18 − 5 − 7
1613 sh	P						
1600 sh	P						
1589 sh	P	1595		1587	w B		
1567 w	P						
1545 s	0.15	1559		1551	m A/B	1542	5 − 7 + 11 + 20
1524 w	P		1519		w		
1467 w	0.32						
1438 sh	P	1447		1438	m B		
1412 s	0.24	1421	1416	1412	m A	1412	20 − 23
1398 m	0.28						
1378 sh	P		1372		w		
1355 w	0.46						
1311 w	0.26					1300	25 + 11 + 13
1305 sh	P	1304	(1298)	1292	m A/B	1296	11 − 23 + 18 − 13
1284 s	0.17	1292		1283	m B	1286	23 − 13 + 21 + 11 − 7
1266 sh	P						
1243 m	0.21	1249	1245	1240	m A	1246	25 − 13 − 11
			1226		w		
1210 m	0.36						
1201 sh							
1184 s	0.32		1174		w	1182	19 + 6 − 13 + 23
1134 m	0.37	1141	1131	1122	m	1133	6 − 19
1123 w	0.52						
		1097		1085	w		
1069 w	0.53						
1021 m	0.29	1034		1025	w B	1020	8
		1014	1006		C		
			1002	993	s C	1003	31 + 36 − 33
1002 w	0.27						
975 w	dp						
962 sh	dp		959		m C	961	30 + 35 − 31
947 m	0.45					943	21 + 19
932 w	0.64	945	937	928	C	936	30 − 28 − 29 − 34
902 m	0.74	914	902	894	s C	901	33 + 36
		908	901		A or C		
874 w	0.34						
864 m	0.75		864	853	C	863	29 − 28
812 w	P						
			802		m C		
794 w	0.59	800	796	792	m A	794	9
759 w	P						
722 m	0.71	730	722	712	s C	724	32
659 w	0.70	664	654	643	m C	654	36 − 31
		609		586	w		
		548	540	533	w		
517 w	0.43	522		514	m B	520	22 − 10 − 12 + 9
508 sh	dp					511	35 − 30
466 w	P		466		w		
437 m	0.11					435	24 + 12 + 6 + 19
422 sh	P						
380 w	0.21						
351 sh	0.42						
332 m	0.35					327	10 + 22
242 w						238	34 + 26 + 27
210 w						213	27 − 26
148 sh						147	12 − 24 − 10 + 22
82 sh						84	26 + 27 − 34
48 m							intermolecular

from the gas phase. For molecules of C_h symmetry where vibrations may be both Raman and infrared active, gas-phase infrared bands are often observed at 5–10-cm^{-1} higher frequencies than corresponding liquid phase Raman bands (see Tables II, III,

TABLE IV: Observed Wavenumbers (cm^{-1}) of Raman Bands of ca. 5 mM (*E*)-1,3,5-Hexatriene-*2,5-d*$_2$ in Ar-Saturated CH_3CN Solution, Excited at 317.5 nm, in the Region 1800–200 cm^{-1}, Together with Calculated Wavenumbers and Potential Energy Distributions of Normal Modes

Raman (solution)	calc wavenumber	calc PED
1618 s	1621	7 − 13 − 25
1571 m	1565	5 + 18 + 8 + 20
1381 m	1379	8 + 20 − 5 − 18
1296 m	1293	13 + 25 + 7
1215 m	1211	9 + 21 − 6 − 19
1023 m	1024	11 + 23 + 9 + 21 + 6 + 19

TABLE V: Observed Wavenumbers (cm^{-1}) and Symmetries of Fundamentals of (*E*)-1,3,5-Hexatriene in the Region 2000–10 cm^{-1},[3] Together with Calculated Wavenumbers and Potential Energy Distributions of Normal Modes

obs	calc	calc PED
		a_g
1628	1631	7 + 5 + 18 − 6 − 19
1574	1576	5 + 18 − 7 + 8 + 20
1397	1395	8 + 20 − 11 − 23
1288	1300	13 + 25 + 11 + 23
1283	1288	11 + 23 − 7 + 9 + 21 + 12 + 24 − 13 − 25
1188	1191	6 + 19 − 9 − 21 + 11 + 23 − 13 − 25
930	931	9 + 21
444	441	12 + 24 + 6 + 19
353	349	10 + 22
		b_g
985	987	30 − 31 + 35 − 36 − 32 + 33
901	904	32 − 33
868	866	28 − 29
615[a]	612	35 − 36 − 30 + 31
215	217	26 − 27
		b_u
1629	1626	5 − 18
1433	1432	8 − 20
1296	1292	11 − 23 − 5 + 18
1255	1257	13 − 25
1132	1133	6 − 19 + 11 − 23
966	959	9 − 21 + 6 − 19
541	544	10 − 22 + 12 − 24
152	154	12 − 24 − 10 + 22
		a_u
1008	1009	30 + 31 + 35 + 36
938	941	34 + 28 + 29
900	899	32 + 33
683	684	35 + 36 − 30 − 31
248	252	34 + 26 + 27
94	87	26 + 27 − 34

[a] From ref 13, crystalline phase.

and VI). These differences shall be discussed further below.

Only in the case of undeuteriated (*E*)-1,3,5-hexatriene can we compare our theoretical results with those of previous calculations. For practically all vibrations, the fit with experiment is improved in our calculation compared to the previous ones. Only for the CH stretches is the improvement limited. Here, however, the assignment of experimentally observed bands is difficult.

Originally, we wanted to include d2345EHT in our force field refinement. However, we found that the vibrational spectra of d2345EHT[17] were incompatible with the spectra of the present study in the refinement, since several d2345EHT bands were calculated by us far from the positions reported from experiment. We thus concluded that the observed spectra of d2345EHT are not only incomplete but also at error with respect to several bands. This view is supported by a remark in BPKP about the possible coexistence of a trideuterio derivative. Consequently, we have not used the d2345EHT spectra at all in the present study.

Frequencies and the Effect of Deuteriation on Normal Modes. CH Stretches. The coupling between CH stretching vibrations involving different internal coordinates seems to be weak. This

TABLE VI: Observed Wavenumbers (cm^{-1}) and Depolarization Ratios of Raman Bands and Wavenumbers and Band Contours of Infrared Bands in the Region 3400–2000 cm^{-1} for (*E*)-1,3,5-Hexatriene (EHT), (*E*)-1,3,5-Hexatriene-*3,4-d*$_2$ (d34EHT), (*E*)-1,3,5-Hexatriene-*3-d* (d3EHT), and (*E*)-1,3,5-Hexatriene-*1,1-d*$_2$ (d11EHT)[a]

Raman (Liquid)

EHT		d34EHT		d3EHT		d11EHT	
	I_{VH}/I_{VV}		I_{VH}/I_{VV}		I_{VH}/I_{VV}		I_{VH}/I_{VV}
3088 m	0.63	3089 m	0.46	3089 m	0.46	3089 m	0.44
3017 w		3015 sh	0.09	3022 sh		3050 w	
3000 m	0.09	2999 s	0.04	3000 m	0.07	3024 sh	0.13
2992 m	0.10	2979 sh	0.41	2994 sh	0.11	2999 m	0.10
		2241 m	0.24	2238 w	0.27	2991 m	0.08
						2363 w	0.34
						2349 w	0.58
						2310 w	0.69
						2216 m	0.11

Infrared (Gas)

EHT contour	d34EHT contour	d3EHT contour	d11EHT contour
3105	3104	3104	3104
3100 s A	3099 s A	3099 s A	3100 m A
3094	3094	3094	3094
3052 m B	3057 w B	3062	3068 sh
3040	3045	3049 w	
		3042	3048 w B
3023	3021		3037
3018 s A	3016 s A	3018 s A/B	
3013	3011	3009	3024 s B
			3014
2969 w[b]	2997 w B	2988	
	2987	2980 sh	2356 sh
		2972	2343
	2974 sh		
		2249 m B	2326 m B
	2252 sh	2238	2315
	2235 m B		2246 sh
	2224		
			2230
			2226 m A
			2221

[a] Only those bands are listed that may be assigned as CH or CD stretches. [b] From ref 13, liquid phase.

is seen from the fact that deuteriation leads to changes in only those modes where the deuterium is directly involved, whereas the remaining modes are changed little. Thus, the calculated EHT modes at 3000 (a_g), 3096 (b_u), and 3037 cm^{-1} (b_u) are found nearly unchanged for d34EHT, d3EHT, and d11EHT, in both theory and experiment; the calculated EHT modes at 3096 (a_g) and 3037 cm^{-1} (a_g) are found nearly unchanged for d34EHT and d3EHT, and the calculated EHT mode at 3025 cm^{-1} (b_u) is found nearly unchanged for d3EHT and d11EHT.

In contrast, CH stretch normal modes involving the same internal coordinates but differing in symmetry (a_g/b_u) show a strong splitting between observed Raman and infrared frequencies, a splitting that is not reproduced in the calculated frequencies. The EHT modes observed at 3017 (a_g) and 3046 cm^{-1} (b_u), the d34EHT modes at 3015 (a_g) and 3051 cm^{-1} (b_u), and even the d3EHT modes at 3022 (a_g-like) and 3049 cm^{-1} (b_u-like) are all calculated at 3037 cm^{-1}. The only way we could lift this discrepancy between theory and experiment was by introducing large coupling constants between CH stretches located at opposite ends of the molecule, which is an unacceptable solution.

CC Stretches. It is seen from Table X that central deuteriation (d34EHT, d3EHT) barely affects the b_u (or b_u-like) C=C (EHT, 1629; d34EHT, 1623; d3EHT, 1628 cm^{-1}; observed) and C–C (EHT, 1132; d34EHT, 1133; d3EHT, 1132 cm^{-1}; observed) stretches. This agrees with expectation, since the central C=C stretch does not contribute to b_u normal modes. For the a_g (or

TABLE VII: Observed Wavenumbers (cm^{-1}) and Symmetries of Fundamentals in the Region 3400–2000 cm^{-1} of (*E*)-1,3,5-Hexatriene (EHT), (*E*)-1,3,5-Hexatriene-*3,4-d*$_2$ (d34EHT), (*E*)-1,3,5-Hexatriene-*3-d* (d3EHT), and (*E*)-1,3,5-Hexatriene-*1,1-d*$_2$ (d11EHT), Together with Calculated Wavenumbers and Potential Energy Distributions of Normal Modes

EHT			d34EHT			d3EHT			d11EHT		
obs	calc	PED	obs	calc	PED	obs	calc	PED	obs	calc	PED
		a_g			a_g			a′			a′
3088	3096	2 + 15 − 1 − 14	3089	3096	2 + 15 − 1 − 14	3099	3096	2 − 15 − 1 + 14	3100	3096	15 − 14
3017	3037	1 + 14 + 2 + 15	3015	3037	1 + 14 + 2 + 15	3089	3096	15 + 2 − 14 − 1	3043	3037	14 + 15
3000	3019	4 + 17	2241	2240	4 + 17	3049	3037	1 + 2 − 14	3024	3025	4 − 17
2992	3000	3 + 16	2999	3000	3 + 16	3022	3037	14 + 15 + 1	3019	3019	17 + 4
		b_u			b_u	3014	3022	17	2999	3001	3 + 16
3100	3096	2 − 15 − 1 + 14	3099	3096	2 − 15 − 1 + 14	3000	3000	3 + 16	2991	2998	16 − 3
3046	3037	1 − 14 + 2 − 15	3051	3037	1 − 14 + 2 − 15	2994	2998	16 − 3	2310	2303	2 − 1
3018	3025	4 − 17	2230	2223	4 − 17	2238	2232	4	2226	2220	1 + 2
	2997	3 − 16	3016	2999	3 − 16						

TABLE VIII: Equilibrium Molecular Structure of (*E*)-1,3,5-Hexatriene Used in the Present Study[a]

C_1H_1, Å	1.075 (1.104)	$H_1C_1C_2$, deg	121.8 (120.5)
C_1H_2, Å	1.072 (1.104)	$H_2C_1C_2$, deg	121.8 (120.5)
C_2H_3, Å	1.077 (1.104)	$C_1C_2C_3$, deg	124.4 (121.7)
C_3H_4, Å	1.077 (1.104)	$C_1C_2H_3$, deg	119.4 (117.0)
C_1C_2, Å	1.329 (1.337)	$H_3C_2C_3$, deg	116.2 (121.3)
C_2C_3, Å	1.460 (1.458)	$C_2C_3C_4$, deg	124.2 (124.4)
C_3C_4, Å	1.334 (1.368)	$C_2C_3H_4$, deg	116.4 (120.6)
$H_1C_1H_2$, deg	116.4 (119.0)	$H_4C_3C_4$, deg	119.4 (115.0)

[a] Experimental values[21] in parentheses.

TABLE IX: Definition of Internal Coordinates; for Atom and Angle Numbering, See Figure 4[a]

		In-Plane	
1	C_1H_1	14	C_6H_8
2	C_1H_2	15	C_6H_7
3	C_2H_3	16	C_5H_6
4	C_3H_4	17	C_4H_5
5	C_1C_2	18	C_5C_6
6	C_2C_3	19	C_4C_5
7	C_3C_4	20	$6^{-1/2}(2\alpha_2 - \beta_{11} - \beta_{12})$
8	$6^{-1/2}(2\alpha_1 - \beta_1 - \beta_2)$	21	$2^{-1/2}(\beta_{11} - \beta_{12})$
9	$2^{-1/2}(\beta_2 - \beta_1)$	22	γ_4
10	γ_1	23	$2^{-1/2}(\beta_9 - \beta_{10})$
11	$2^{-1/2}(\beta_4 - \beta_3)$	24	γ_3
12	γ_2	25	$2^{-1/2}(\beta_7 - \beta_8)$
13	$2^{-1/2}(\beta_6 - \beta_5)$		
		Out-of-Plane	
26	τ	$^1/_2(C_1C_2C_3C_4 + H_3C_2C_3C_4 + C_1C_2C_3H_4 + H_3C_2C_3H_4)$	
27	τ	$^1/_2(C_3C_4C_5C_6 + H_5C_4C_5C_6 + C_3C_4C_5H_6 + H_5C_4C_5H_6)$	
28	ω	$(C_4C_2C_3H_4)$	
29	ω	$(C_3C_5C_4H_5)$	
30	ω	$(C_1C_3C_2H_3)$	
31	ω	$(C_6C_4C_5H_6)$	
32	ω	$(H_2H_1C_1C_2)$	
33	ω	$(H_7H_8C_6C_5)$	
34	τ	$^1/_2(C_2C_3C_4C_5 + C_2C_3C_4H_5 + H_4C_3C_4C_5 + H_4C_3C_4H_5)$	
35	τ	$^1/_2(H_2C_1C_2C_3 + H_2C_1C_2H_3 + H_1C_1C_2C_3 + H_1C_1C_2H_3)$	
36	τ	$^1/_2(C_4C_5C_6H_7 + C_4C_5C_6H_8 + H_6C_5C_6H_7 + H_6C_5C_6H_8)$	

[a] The out-of-plane coordinates are defined according to ref 26; for the torsional coordinates (τ), this definition is identical with that of ref 27. For internal coordinate 28, hydrogen out-of-plane bending (ω), C_4 and C_2 are anchor atoms, C_3 is apex atom, and H_4 moves down below the plane of the paper; internal coordinates 29–31 are defined accordingly. For internal coordinate 32, H_2 and H_1 are anchor atoms, C_1 is apex atom, and C_2 moves down below the plane of the paper; internal coordinate 33 is defined accordingly.

a_g-like) modes, the C=C stretches are lowered (EHT, 1628 and 1574; d34EHT, 1607 and 1565; d3EHT, 1616 and 1559 cm^{-1}; observed) and the C–C stretches raised (EHT, 1188; d34EHT, 1201; d3EHT, 1203 cm^{-1}; observed) by central deuteriation. For d25EHT, a similar pattern is seen, but here the a_g modes are affected little, whereas the b_u modes shift. Thus, coupling with the CH rocks pushes upward the C=C stretches and downward the C–C stretches.

CH_2, CH, CCC In-Plane Deformations. For d11EHT we find the CH_2 scissoring at 1412 cm^{-1}. This is close to the average of the a_g and b_u CH_2 scissorings found in EHT, d34EHT, and d3EHT. The CH_2 scissorings in d25EHT are lowered compared to EHT, d34EHT, and d3EHT, a sign that the CH rock at C_2 couples with the neighboring CH_2 scissoring and pushes it upward.

The 1296-cm^{-1} (EHT, observed) b_u normal mode is quite unaffected in d34EHT, d3EHT, and d11EHT and must thus belong to the CH rock at C_2, whereas the 1255-cm^{-1} b_u mode must belong to the CH rock at C_3. The 1283-cm^{-1} (EHT; observed) a_g normal mode is nearly unchanged in d34EHT, d3EHT, and d11EHT and must belong to the CH rock at C_2. Generally, there is a strong coupling between CD rock and CH_2 rock. For d11EHT, the CH_2 rock is found at 947 cm^{-1}, close to the average of 966 and 930 cm^{-1} from EHT. Among the CCC deformations, only the b_u central deformation (EHT, 152 cm^{-1}, observed) is unaffected by deuteriation.

Out-of-Plane Vibrations. For the out-of-plane vibrations, the terminal CH_2 wags are influenced by deuteriation in d11EHT and d25EHT, but not in d34EHT and d3EHT, whereas the CH wags are changed little by the terminal deuteriation in d11EHT compared to EHT. Generally, only those CH wags being directly deuteriated are shifted substantially. These observations can be interpreted by assuming that the range of coupling between the CH/CH_2 out-of-plane wags is quite short, being efficient only for wags situated on neighboring carbon atoms. This empirical observation is supported by remarks below about the out-of-plane force field.

The vibrations that are dominated by terminal C=C torsion are influenced strongly by central (d34EHT) and, especially terminal (d11EHT) deuteriation, whereas the C–C torsions generally are influenced little by deuteriation.

In-Plane Force Field. The ab initio force field of BPKP was calculated at the HF/6-31G level. Subsequently, the diagonal force constants were scaled to improve the fit with the experimentally observed frequencies. The same force field was also the basis of YFT, but here the scaling factors were different. The ab initio force field of FSLBP was calculated at the HF/4-21G level and subsequently scaled. The ab initio force field of SKL was calculated at the SCF level with DZ+P and TZ+P basis sets and subsequently scaled. In the present study, we used the scaled force field of BPKP as the starting point in our force field refinement. We shall now look closer at the modifications resulting from our refinement, as listed in Table XI for the in-plane force field.

Among the diagonal force constants connected with the CH (CD) stretches, only one is changed appreciably in the present study; for the C_2H_3 stretch the force constant is lowered by about 2%. This lowering seems reasonable, since our calculated normal modes dominated by C_2H_3 stretch generally agree quite well with experiment. Moreover, the coupling between the C_1H_1 and C_1H_2 stretches is increased in our final force field. The scaling factors for the CH stretch diagonal force constants were not changed between BPKP and YFT but were increased in FSLBP.

The diagonal force constants for the CC stretches are all increased in our refinement, especially the one for the terminal C=C

TABLE X: Calculated and Observed Wavenumbers (cm^{-1}) and Symmetries of Normal Modes of Vibration of (*E*)-1,3,5-Hexatriene (EHT), EHT-*3,4*-d_2 (d34EHT), EHT-*3*-*d* (d3EHT), EHT-*1,1*-d_2 (d11EHT), and EHT-*2,5*-d_2 (d25EHT)

EHT			d34EHT			d3EHT		d11EHT		d25EHT		
obs		calc	obs		calc	obs	calc	obs	calc	obs		calc
						In-Plane						
						a′		a′				
3100	b_u	3096	3099	b_u	3096	3099	3096	3100	3096		b_u	3095
3088	a_g	3096	3089	a_g	3096	3089	3096	3043	3037		a_g	3095
3046	b_u	3037	3051	b_u	3037	3049	3037	3024	3025		b_u	3037
3018	b_u	3025	3016	b_u	2999	3022	3037	3019	3019		a_g	3037
3017	a_g	3037	3015	a_g	3037	3014	3022	2999	3001		b_u	3023
	b_u	2997	2999	a_g	3000	3000	3000	2991	2998		a_g	3019
3000	a_g	3019	2241	a_g	2240	2994	2998	2310	2303		a_g	2219
2992	a_g	3000	2230	b_u	2223	2238	2232	2226	2220		b_u	2216
1629	b_u	1626	1623	b_u	1623	1628	1626	1633	1630	1618	a_g	1621
1628	a_g	1631	1607	a_g	1607	1616	1616	1618	1612		b_u	1608
1574	a_g	1576	1565	a_g	1563	1559	1571	1545	1542	1571	a_g	1565
1433	b_u	1432	1425	b_u	1427	1428	1429	1412	1412		b_u	1418
1397	a_g	1395	1396	a_g	1394	1397	1394	1311	1300	1381	a_g	1379
1296	b_u	1292	1294	b_u	1291	1296	1293	1298	1296	1296	a_g	1293
1288	a_g	1300	1285	a_g	1291	1288	1291	1284	1286		b_u	1255
1283	a_g	1288	1201	a_g	1203	1266	1267	1245	1246	1215	a_g	1211
1255	b_u	1257	1133	b_u	1140	1203	1204	1184	1182		b_u	1183
1188	a_g	1191	1044	b_u	1033	1132	1136	1131	1133	1023	a_g	1024
1132	b_u	1133	1001	a_g	1000	1024	1021	1021	1020		b_u	985
966	b_u	959		b_u	875	938	943	947	943		b_u	884
930	a_g	931	871	a_g	861	875	868	796	794		a_g	858
541	b_u	544	512	b_u	513	525	528	517	520		b_u	538
444	a_g	441	438	a_g	434	441	437	437	435		a_g	423
353	a_g	349	345	a_g	342	350	345	332	327		a_g	344
152	b_u	154	151	b_u	152	151	153	148	147		b_u	150
						Out-of-Plane						
						a″		a″				
1008	a_u	1009	992	a_u	999	1009	1002	1002	1003		a_u	958
985	b_g	987	984	b_g	986	996	987	962	961		b_g	932
938	a_u	941	902	a_u	900	909	906	932	936		a_u	930
901	b_g	904	901	b_g	903	902	901	902	901		b_g	870
900	a_u	899	787	b_g	789	895	895	864	863		a_u	798
868	b_g	866	736	a_u	734	770	771	722	724		b_g	788
683	a_u	684	658	a_u	656	681	680	654	654		a_u	682
615	b_g	612	558	b_g	561	(580)	575	508	511		b_g	595
248	a_u	252	247	a_u	247	252	251	242	238		a_u	220
215	b_g	217	201	b_g	202	213	208	210	213		b_g	214
94	a_u	87	87	a_u	86	83	86	82	84		a_u	86

TABLE XI: In-Plane Force Constants for (*E*)-1,3,5-Hexatriene and Deuteriated Derivatives, Refined in the Present Study[a]

		F_{ij}				
i	*j*	BPKP[b]	YFT[c]	FSLBP[d]	SKL[e]	this work
1	1	5.092	5.094	5.1472		5.093
2	2	5.164	5.166	5.2115		5.160
3	3	5.000	4.997	5.0669		4.911
4	4	4.984	4.986	5.0530		4.978
5	5	8.127	8.136	8.6134	8.344	8.407
6	6	4.957	5.061	5.0677	5.042	4.999
7	7	7.882	7.891	8.3881	8.076	8.028
8	8	0.451	0.446	0.4518		0.433
9	9	0.532	0.526	0.5258		0.517
10	10	1.066	1.053	1.0434		1.071
11	11	0.533	0.528	0.5264		0.514
12	12	1.068	1.056	1.0510		1.198
13	13	0.483	0.500	0.5250		0.501
1	2	0.026	0.026	0.0329		0.062
5	6	0.318	0.322	0.3793	0.469	0.488
5	7	−0.081	−0.081	−0.0938	−0.146	−0.158
5	19	0.035	0.035	0.0424	0.050	0.124
6	7	0.294	0.297	0.3507	0.430	0.311
6	19	−0.053	−0.054	−0.0600	−0.063	−0.248

[a] Units are mdyn/Å for diagonal stretch constants and stretch–stretch interactions and mdyn Å/rad^2 for diagonal bend constants. The remaining in-plane force constants were unchanged from BPKP.[11] [b] Reference 11. [c] Reference 28. [d] Reference 12. [e] Reference 14.

bond. This is increased by 3.4%, for the C–C stretch the increase is 0.8%, and for the central C=C stretch the increase is 1.9%. Our refined CC stretch diagonal force constants agree well with those of SKL. The scaling factors for the C=C stretches were barely changed between BPKP and YFT, whereas that of C–C stretch was increased by 2%. Our study supports the view that the terminal C=C bonds in (*E*)-1,3,5-hexatriene are stronger, and consequently shorter, than the central one.

In our refinement, all coupling constants between CC stretches are increased numerically. This is in agreement with the view proposed by YFT that interaction force constants between skeletal stretching coordinates are underestimated in absolute value[13] and the view proposed by SKL that inclusion of electron correlation leads to an increase in absolute value of all CC stretch–stretch coupling constants.[14]

It is interesting to note the agreement between our refined CC stretch coupling constants and those of SKL. However, our value for the coupling constant between the C–C stretches is numerically larger than in any of the previous studies. The correctness of our analysis is supported by the agreement between our calculated and observed frequencies of the C–C stretches.

The diagonal force constants corresponding to internal coordinates 9 (CH_2 rock) and 11 (CH rock) are decreased by about 3% in our refinement; the one corresponding to internal coordinate 13 (CH rock) is increased by a similar amount. This has the effect of bringing closer together the force constants connected with CH in-plane rock. It is particularly remarkable that the force constants connected with the CH rocks at C_2 and C_3 are brought much closer to each other. These changes are qualitatively the same as the changes from BPKP to YFT, but the changes in the present study are larger. The three CH rock diagonal force constants of FSLBP are even closer to each other than in our study.

TABLE XII: Out-of-Plane Force Field for (E)-1,3,5-Hexatriene and Deuteriated Derivatives[a]

		F_{ij}			
i	j	BPKP[b]	YFT[c]	FSLBP[d]	this work
26	26	0.025	0.035	0.0331	0.0366
28	28	0.243	0.236	0.2485	0.2714
30	30	0.255	0.248	0.2603	0.2813
32	32	0.238	0.230	0.2438	0.2321
34	34	0.118	0.117	0.1167	0.0949
35	35	0.123	0.122	0.1218	0.1099
26	27	0.000	0.000	−0.0002	0.0000
26	28	−0.002	−0.003	0.0044	−0.0020
26	29	0.000	0.000	0.0001	0.0000
26	30	−0.002	−0.002	−0.0036	−0.0020
26	31	0.000	0.000	0.0000	0.0000
26	32	0.000	0.000	0.0002	0.0000
26	33	0.000	0.000	−0.0001	0.0000
26	34	0.005	0.006	0.0052	0.0132
26	35	0.004	0.004	0.0042	0.0177
26	36	0.000	0.000	−0.0004	0.0000
28	29	0.021	0.021	0.0243	0.0515
28	30	−0.009	−0.009	0.0116	−0.0090
28	31	−0.004	−0.004	0.0051	−0.0187
28	32	−0.003	−0.004	0.0045	−0.0140
28	33	−0.001	−0.001	0.0016	−0.0010
28	34	0.000	0.000	−0.0004	0.0000
28	35	0.013	0.013	−0.0144	0.0186
28	36	0.005	0.005	−0.0051	0.0006
30	31	0.003	0.003	0.0031	0.0004
30	32	0.025	0.024	0.0290	0.0122
30	33	0.001	0.001	0.0012	0.0010
30	34	0.014	0.013	0.0147	0.0324
30	35	0.000	0.000	0.0000	0.0000
30	36	−0.002	−0.002	−0.0020	−0.0020
32	33	0.000	0.000	0.0004	0.0000
32	34	0.005	0.005	0.0051	0.0038
32	35	0.001	0.000	0.0005	0.0010
32	36	−0.001	−0.001	−0.0008	−0.0010
34	35	−0.005	−0.005	−0.0059	−0.0019
34	36	−0.005	−0.005	−0.0059	−0.0019
35	36	0.001	0.001	0.0013	0.0010

[a] Units are mdyn Å/rad². [b] Reference 11. [c] Reference 28. [d] Reference 12.

For the diagonal force constats connected with CCC in-plane deformation, the situation is reversed. In the initial force field,[11] internal coordinates 10 and 12 are close together, whereas in our refinement, 10 is left nearly unchanged and 12 is increased by as much as 12%. This change seems to be correct, since the agreement with experiment is improved strongly for the four lowest in-plane modes that are quite pure CCC deformations. The CCC force constants are barely changed among BPKP, YFT, and FSLBP.

Out-of-Plane Force Field. Among the diagonal out-of-plane force constants listed in Table XII, those connected with C–C torsion, internal coordinates 26 and 27, are increased in our refinement. The refined value, 0.0366, is close to those obtained by YFT and FSLBP. The force constants connected with C=C torsion, internal coordinates 34, 35, and 36, are decreased. Here, the central C=C torsion force constant (34) is decreased more than the terminal C=C torsion ones (35, 36), again indicating a weakening of the central C=C bond compared to the terminal ones. The force constants for the CH out-of-plane wags, internal coordinates 28–31, are increased. The diagonal force constants connected with C=C torsion and CH wag of YFT and FSLBP are close to those of BPKP. For the CH_2 wags, internal coordinates 32 and 33, the diagonal force constants of the present study are close to those of BPKP, YFT, and FSLBP.

For the out-of-plane interaction force constants, the absolute size of the changes resulting from our refinement is small, but the relative changes are large. However, none of the interaction constants change sign between BPKP and the present calculation. There is a tendency in the changes, such that interactions between internal coordinates that are close to each other in the molecule tend to increase, whereas interactions between internal coordinates that are further from each other tend to decrease. Thus, our calculation shows larger values and a shorter range for the interaction force constants between out-of-plane vibrations. This was also observed experimentally above. It should be noted that this tendency also holds for torsional interactions. In particular, the long-range interactions between CC torsions do not increase as one might expect from the results for the in-plane force field.

Acknowledgment. We thank Kort- og Matrikelstyrelsen for generously putting their RC 8000 computer at our disposal. Drs. O. F. Nielsen, F. M. Nicolaisen, and G. O. Sørensen, Chemical Laboratory V, H. C. Ørsted Institute, University of Copenhagen, are gratefully acknowledged for help with Raman and infrared spectra and calculations. We thank professor M. Tasumi for communicating to us the full force field of ref 13. This work was supported by the Danish Natural Science Research Council (Grant 11-6151) and a collaborative research grant from NATO (Grant 0137/88).

Registry No. EHT, 821-07-8; D, 7782-39-0.